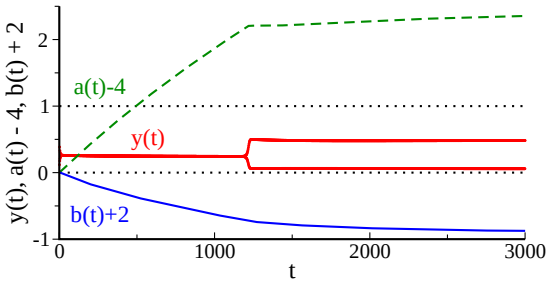

FIG. 3: (color online) The time dependence of $y(t)$ (red stars) $b(t)+2$ (solid line) and of $a(t)-4$ (dashed line) for the one-site problem with inhibitory self-coupling $x \to 1/2 - y$, $\epsilon_a = \epsilon_b = \epsilon = 0.01$ and $\mu = 0.28$. A Hopf-bifurcation occurs for the output $y(t)$ when the initial quasistationary fixpoint becomes unstable, giving place to a new fixpoint of period two.

Evaluating the local Lyapunov exponents we find that the trajectory is stable against perturbations for the transient states close to one of the transient fixpoints of $y = g(a[y-1/2]+b)$ and sensitive to perturbations and external modulation during the fast transition periods, an instantiation of the general notion of transient state dynamics [10, 11].

Inhibitory self-coupling.– So far we discussed, see (5) and Fig. 2, a neuron having its output $y(t)$ coupled back excitatorily to its input via $x \to y - 1/2$. The dynamics changes qualitatively for an inhibitory self-coupling $x \to 1/2 - y$, see Fig. 3. There is now only a single intersection of $g(a[-y+1/2]+b)$ with y. This intersection corresponds to a stable fixpoint for small gains a. A Hopf-bifurcation [14] occurs when $a(t)$ exceeds a certain threshold and a new fixpoint of period two becomes stable. The coordinates of this fixpoint of period two slowly drift, compare Fig. 3, due to the residual changes in $a(t)$ and $b(t)$. Interestingly, the dynamics remains non-trivial, as a consequence of the continuous adaption, even in the case of inhibitory self-coupling.

Self organized chaos.– We have studied numerically fully connected networks of $i = 1, .., N$ polyhomeostatically adapting neurons (4), coupled via

$$x_i(t) \;=\; \textstyle\sum_{j \neq i} w_{ij} y_j(t) \;. \qquad (8)$$

The synaptic strengths are $w_{ij} = \pm 1/\sqrt{N-1}$, with inhibition/excitation drawn randomly with equal probability. The adaption rates are $\epsilon_a = \epsilon_b = 0.01$. We consider homogeneous networks where all neurons have the identical μ for the target output distributions (2), with $\mu = 0.15$, 0.28 and $\mu = 0.5$.

The activity patterns presented in the inset of Fig. 4 are chaotic for the $\mu = 0.28$ network and laminar with intermittent bursting for the network with $\mu = 0.15$. This behavior is typical for a wide range of network geometries, distributions of the synaptic weights and for all initial conditions sampled. The respective Kullback-Leibler divergences D_λ decrease with time passing, as shown in

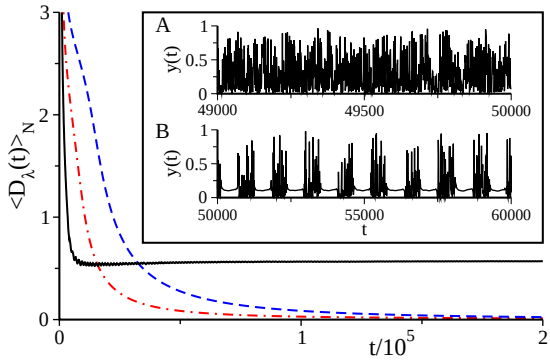

FIG. 4: (color online) Mean Kullback-Leibler divergence D_λ, for $N = 500$ networks, of the real and target output distributions as a function of number of iterations t. The solid black, dashed-dotted red and the dashed blue lines correspond respectively to target firing rates $\mu = 0.15$, $\mu = 0.28$, and $\mu = 0.5$. Inset: Output activity of two randomly chosen neurons for target average firing rates $\mu = 0.28$ (top) and $\mu = 0.15$ (bottom).

Fig. 4, due to the ongoing adaption process (4). D_λ becomes very small, though still finite, for long times in the self-organized chaotic regime ($\mu = 0.28$, 0.5), remaining substantially larger in the intermittent bursting phase ($\mu = 0.15$).

We have evaluated the global Lyapunov exponent, [15] finding that two initial close orbits diverge until their distance in phase space corresponds, within the available phase space, to the distance of two randomly selected states, the tellmark sign of deterministic chaos. [14] The corresponding global Lyapunov exponent is about 5% per time-step for $\mu = 0.5$ and initially increases with the decrease of μ, until the intermittent-bursting regime emerges, after which the global Lyapunov exponent declines with the decrease of μ.

The system enters the chaotic regime, in close analogy to the one-side problem discussed previously, whenever the adaptive dynamics (4) has pushed the individual gains $a_i(t)$, of a sufficient number of neurons, above their respective critical values. Hence, the chaotic state is self-organized. Chaotic dynamics is also observed in the non-adapting limit, with $\epsilon_a, \epsilon_b \to 0$, whenever the static values of a_i are above the critical value, in agreement with the results of a large-N mean field analysis of an analogous continuous time Hopfield network. [16] Subcritical static a_i lead on the other side to regular dynamics controlled by point attractors.

In Fig. 5 we present the distribution of the output activities for networks with target mean firing rates $\mu = 0.28$ and $\mu = 0.5$. Shown are in both cases the firing rate distributions $p(y)$ of the two neurons having respectively the largest and the smallest Kullback-Leibler divergence (3) with respect to the target exponential distributions (2). Also shown in Fig. 5 are the distributions of the network-averaged output activities.